FLATNESS ERROR DIAGNOSTICS IN FACE MILLING OF AOD AND AODI TRANSMISSION PARTS

By
S.G. Chen
A.G. Ulsoy
Y. Koren

Final Report to the Ford Motor Co.
Technical Report #UM-MEAM-90-08

Department of Mechanical Engineering
The University of Michigan, Ann Arbor
11/20/90

TABLE OF CONTENTS

LIST OF FIGURES

I. INTRODUCTION

Face milling is used in the manufacture of AOD and AODI transmission parts(Fig. 1) to produce mating surfaces with flatness errors less than three ten-thousands inch in order to ensure good transmission performance. The AODI part manufacturing process has been modified from the previously produced AOD part. A new milling machine, new milling cutters, and new cutting conditions are used. The new AODI part is to be studied for possible error sources which make it difficult to meet the above flatness requirement. The new process is high speed (5000rpm) and uses a smaller diameter (7.5" instead of 15") cutter. Instead of a single roughing and single finishing pass as in the AOD, the AODI process uses "s" patterned roughing and "u" patterned finishing passes.

In this study, three possible error sources have been investigated: (1)the geometric error of the machine tool due to spindle alignment, (2) the deflection of the transmission part due to the cutting force, and (3) the thermal expansion of the part during cutting.

The machine tool used for the milling tests was a Fadal CNC 80 Milling Machine Center (Fig. 2), which is located in Department of Mechanical Engineering, the University of Michigan, Ann Arbor, Michigan. The same testing procedures used at U.M. for identifying the machine tool geometric error will also be repeated at Ford's transmission plant, Livonia, Michigan.

II. OBJECTIVES

The objective of this work was to

1. Study three possible sources contributing to the flatness error of the AODI transmission: (1) geometric errors of the spindle, (2) deflections of the transmission part caused by the axial cutting force, and (3) thermal deformations of the transmission part during cutting.

2. Investigate the major cause of the flatness problem in the face milling process of AOD/AODI transmission cases.

3. Make recommendations for improving the flatness of the face milling operations used in manufacturing the AOD/AODI transmission cases.

III. TECHNICAL APPROACH

In accordance with the above objectives, the following technical approaches have been used:

A. **Analyses of geometric errors, milling forces, and thermal deformations:** Before any machining test, (1) the geometric error of the machine tool was predicted by measuring the spindle tilt with a dial gage indicator; (2) the milling forces were simulated by using the mechanistic model proposed by Fu, et al[4]; then, the thermal deformation of the transmission part were predicted by using a lumped temperature model developed by Chen [6].

B. **Milling test to evaluate machine geometric errors:** The geometric error of the machine tool due to spindle tilt was evaluated by measuring the flatness of a face-milled plate (See Fig. 9 for measurement examples.)

C. **Test to evaluate deflections of the transmission case caused by the axial cutting force:** The deflection of an AODI case was measured under a static load of the same magnitude as the simulated axial milling force.

D. **Thermal Deflection Analysis and Cutting Experiments:** During the milling process, the thermal deformation of the transmission part was calculated from the measured temperature distribution of the part. Temperature measurements were made in the following cutting

experiments: (1) dry cutting, (2) cutting with room-temperature coolant, and (3) cutting with coolant at 30°F below room temperature.

A. Analyses of Geometric Errors, Milling Forces, and Thermal Deformations

1. Machine Geometric Errors Using a Dial Gage indicator

In the flatness problem of face milling, the machine geometric errors are assumed to be dominated by spindle tilt (Fig. 4). In order to identify the degree of spindle tilt, a dial-gage indicator of resolution (.0005/4)" and measurement radius of 6.5" has been used to identify the spindle orientation with respect to the machine table. The relative height of the machine table to a reference point was measured by rotating the indicator on the table. Measured results are depicted in Figure 5 (the circle diameter is 13"). From Figure 5 and the tool path (Fig. 13), the effective tilting was estimated as

$$\beta = \frac{\text{height difference}}{\text{diameter}} \quad \text{(similar to Figure 4)}$$

$$= \frac{.0005"}{13"} = 3.84*10^{-5} \text{ radians} \pm 0.96*10^{-5} \text{ radians},$$

which will cause a step of (7.48*ß)"=(280±70) μ-inches. This predicted number will later be compared with measured results.

2. Simulation of Milling Forces

Since it is very difficult to simulate the actual cutting force due to the transmission part's complicated geometry, it is very important to simulate the milling force on a flat plate. Indeed, the plate-milling force is an upperbound force, since

the worm holes in the transmission case reduce the chip load (and consequently the force) compared to a solid plate

Figure 6 shows the face milling process for a flat plate. The method of force calculation(Fu, et al., [4]) is to accumulate all the cutting forces contributed by each blade and then to calculate the total force acting on the cutter using a coordinate transformation.

2.1. Finishing Force

After simulating the milling force for finishing of a flat plate (Fig. 7), the actual cutting force components are assumed to be bounded by

$|Fx| \leq 10.71$ lb,

$|Fy| \leq 22.3$ lb,

and $|Fz| \leq 4.3$ lb.

Thus, $Fz=4.3$ lb is then used as the load in the static force-deflection test. Again, due to the worm holes, the actual forces on the transmission will be smaller. Thus, the above values are expected to yield upperbound values of the static deflections in the actual part.

2.2. Roughing Force

From the results in Figure 8, the real cutting force components are assumed to be bounded by

$|Fx| \leq 41.21$ lb,

$|Fy| \leq 91.37$ lb,

and $|Fz| \leq 16.34$ lb.

These values are, once again, upper bound values.

3. Thermal Deformations of the Transmission Case Using a Lumped Temperature Model

In order to calculate the machining error due to thermal effects, the temperature rise of the case in dry cutting was first calculated by modeling the transmission case as a lumped system (Chen, [6]). Then, using the workpiece dimensions, the thermal deformation of the workpiece was calculated.

3.1. Cutting Temperature of the Transmission Case

Since the temperature distribution in the workpiece is rather uniform except near the shear plane([2],pp 283), it has been assumed to be a uniform temperature distribution. Then, a simple formula ([6]) based on this assumption was used to calculate the temperature rise for a short time period of cutting. The calculation yields,

$$\theta_T = \frac{R_w F_{yo} V_o}{MC} t = \frac{R_w * (\text{cutting power}) * t}{MC}$$

$$= \frac{0.1 * (6250\,W) * (12\,sec.)}{32 * .454\,kg * 963 \frac{J}{kg}\,K}$$

$$= 0.536\ K$$

where the cutting power is simulated as shown in Figure 7 using the model in [4].

Rw: Percentage of the cutting power flowing into the workpiece. Rw ≈10 % for high speed machining (Shaw, [2])

θ_T: temperature rise of the workpiece.

C: specific heat of the workpiece.

α: thermal expansion coefficient.

Vo: steady cutting speed (m/min).

Fyo: nominal cutting force (N).

t: cutting time (sec).

3.2. Thermal Deformations of the Transmission Case

The thermal deformation can then be calculated using the following formula:

$$\text{thermal deformation} = \alpha * \theta_T * H$$

$$= (21.5 * 10^{-6} \frac{1}{^oK}) * (0.536\ ^oK) * (4 * .0254\ m)$$

$$= 1.86\ \mu m$$

$$= 73\ \mu\text{-inches}$$

where H is the height of the workpiece (approximately 4", see Appendix).

B. Milling Test to Evaluate Machine Geometric Errors: Face Milling on a Flat Plate

1. Evaluation of Geometric Errors by Measuring the Flatness of a Face-Milled Flat Plate

The machine tool error has been evaluated by milling a flat plate mounted on the case (Fig.10). The cutting conditions (see Appendix) and the directions of tool motion were chosen to be the same as in finishing an AODI case. A "u" patterned finishing pass (Fig. 9) was used so as to duplicate the machine tool geometric error in milling the transmission case.

2. Experimental Design And Setup

The flat plate was chosen to be a cast aluminum tooling plate with hardness number HB=67, which is close to the one used in the casting of the transmission parts (HB=70). Figure 10 shows that the plate is mounted on an AOD case.

3. Experimental Results

From the measured results (Figure 9), the maximum step error is about 300±50 μ-inches.
As a comparison, given the machined surface profile(Fig. 22) from Ford's transmission plant, there is also a maximum step of about the max. height 300±50 μin.

C. Test to Evaluate Deflections of the Transmission Case Caused by the Axial Cutting Force

1. Evaluation of the Transmission Deflection Using the Static Force-Deflection Test

The static force-deflection test has been done to simulate the part deflection caused by the axial milling force. Here the deflection of an AODI case was measured under a load of the same magnitude as the simulated axial milling force.

2. Experimental Design and Setup

In the force-deflection experiment, we tried to simulate the vertical cutting force component and to measure this force component and the workpiece deflections. Figure 11 shows the schematic of the experiment. The force was given by a known weight, and the deflection is measured by a proximity probe, which is a non-contacting sensor with a high resolution (up to 1 μm). After calibrating the proximity probe (Fig. 12), we have a sensitivity of about $6.75^{*}\ 10^{-4}\ \frac{\text{Volts}}{\mu\text{-inches}}$ at a distance of around 0.012".

3. Experimental Results

Various loads are applied on each selected deflection point. The load will be increased from zero up to 10 pounds, even though the estimated axial force component (Fz) is at most 4.3

lb. The maximum voltage change under a 10 lb load is .05 Volts. Then the maximum deflection was calculated as

$$\frac{\text{voltage change}}{\text{sensitivity}} = \frac{0.05}{6.75 * 10^{-4}} \approx 75 \ \mu\text{-in.}$$

The deflections measured at 6 points (Fig. 11, the points marked from 1 to 6) under a 10 lb load were all less than 75 μ-inches. Consequently, *the maximum deflections expected due to axial loads less than 4.3 lbs in the machining operations are expected to be less 35 μ-in.*

D. Thermal Deformation Analysis and Cutting Experiments

1. Evaluation of the Thermal Deformation by Measuring the Cutting Temperature of the Transmission Part

The thermal deformations of the transmission case during cutting have been studied by measuring the temperature distribution of four specific locations, i.e., the points marked A, B, C, and D shown in Figure 13. The temperature distribution has been measured by placing thermocouples underneath each mark (Fig. 14). Three different cutting environments have been utilized: (1) dry cutting, (2) cutting with coolant at room temperature, and (3) cutting with coolant $30^{o}F$ below room temperature.

1.1. Dry Cutting

For the case of dry cutting, the cutting temperature when the cutter touched the marked point was assumed to be the maximum temperature measured by the thermocouple beneath the marked point (Fig. 17). The temperature distribution was then expressed in terms of x, the distance below the cutting surface. After proceeding with the finishing cut for several times, i.e., cutting with various x's, the temperature rise of each point (i.e., A, B, C, and D) in terms of x (i.e., $\Delta T=\Delta T(x)$) was obtained, then used to calculate the thermal deformation from [6]:

$$\text{thermal deformation} = \alpha \int_0^{\infty} \Delta T(x)dx \ ,$$

where α is the thermal expansion coefficient and ΔT is the temperature rise when the cutter reaches the measured point.

1.2. Cutting with Coolant at Room Temperature

In this case, the procedures for evaluating the temperature distribution and the thermal deformation were exactly the same as in dry cutting.

1.3. Cutting with Coolant 30°F below Room Temperature

Because of the "cold" coolant's cooling effect, the temperature of the marked point (for example, A) when the cutter reaches the point will no longer be the highest measured temperature (Fig. 20).

Therefore, the temperature was obtained at the instant when the cutter reached the marked point. By refering to the measured temperatures in dry cutting, we were able to determine when the cutter reached the points A, B, C, and D. Then we select the measured data at the these moments as the temperatures when the cutter reached A, B, C, and D. However, this method is only an estimate. The temperature distribution obtained is, thus, approximate.

In order to estimate the thermal deformation more conservatively, the solution of a one-dimensional transient conduction problem was used to "bound" the measured temperatures and was used to calculate the thermal deformation.

The one-dimensional transient conduction problem considering the effect of "cold" coolant was formulated and solved as follows:

<u>one-dimensional conduction problem</u>:

<u>equation</u>: $$\frac{\partial(\Delta T)}{\partial t} = a\frac{\partial^2(\Delta T)}{\partial x^2},$$

<u>Initial conditions</u>: $\Delta T(0,0)=-DT$, $\Delta T(x,0)=0$ for all x's >0,

(The original temperature of the transmission case was the same as room temperature and, a sudden boundary temperature change -DT was caused by adding "cold" coolant.)

Temperature distribution $= \Delta T=-DT\cdot e^{-\frac{x^2}{a\,t}}$

Thermal deformation $=\alpha\int_0^{\infty}\Delta T(x)dx= -DT\alpha\sqrt{\frac{a\,t}{2}}$

where $\Delta T(x,t)$= temperature variation of the part,
a = diffusivity of Aluminum,
α = thermal expansion coefficient of Aluminum,
DT=temperature difference between the part and coolant before cutting,
t = the time when the cutter touches the selected point.

Therefore, the "bound" temperature distribution was of the form $-e_3 \cdot e^{-e_4 \cdot x^2}$, where e_3 and e_4 are chosen constants.

2. Experimental Design and Setup

The experimental design is shown in Figure 13. Part (a) shows the top view of the machined surface and the cutter contour. The four points (A, B, C, and D) were selected for thermal expansion calculations. Part (b) shows the distance (x) between the measured point and the cutter. When the cutter reached the selected point, the measured temperature was denoted as T=T(x).

The placement of thermocouples is shown in Figure 14. Several tiny holes underneath the selected points were drilled to insert the thermocouples so as to measure the cutting temperature in the workpiece.

The setup for the cutting temperature measurement is shown in Figure 15. The case temperature was measured by 8 E-type thermocouples so as to obtain fast temperature measurements. The measured analog signals were sent to the computer via the temperature measuring circuit and the A/D converter. The sampling interval was one second.

The resolution of the temperature measuring system is approximately one degree Centigrade. Figure 16 shows the typical measured temperatures before cutting.

3. Experimental Results

3.1. Dry Cutting

For the case of dry cutting, the typical measured temperatures are depicted in Figure 17.

From the measured results of Figure 17, the measured distributions for each select point are shown in Figure 18. The distribution of temperature rise $\Delta T(x)$ was approximated by a simple linear formula, $\Delta T(x)=e_1-e_2x$, so as to calculate the thermal expansion.

The calculation results are tabulated as follows:

	A	B	C	D
e_1	3.5218	2.9931	1.9977	4.043
e_2	0.096284	0.0395	0.079702	0.1512
thermal expan. (μm)	1.4	2.4	0.5	1.2
thermal expan.(μ-inch)	55	96	21	46

therefore, *the maximum deformation was less than 100 μ-in.*

3.2 Cutting with Coolant at Room Temperature

The typical measured temperatures are depicted in Figure 19. When compared with the temperatures in dry cutting (Fig. 17), the thermal expansions in this case was always less than the results in dry cutting, i.e., *the maximum deformation was less than 100 μ-in.*

3.3. Cutting with coolant at 30°F below Room Temperature

The typical measured temperatures are depicted in Figure 20. Measured temperature distributions for points A, B, C, and D are shown in Figure 21. The "bound" temperature distribution was chosen to be

$$\Delta T = -e_3 \cdot e^{-e_4 \cdot x^2}$$

with $e_3 = 17^{\circ}F = 9.44^{\circ}C$ and $e_4 = 0.0034 \frac{1}{mm^2}$ (Fig. 21). The corresponding thermal deformation was then calculated -96 μin. (-2.45μm). Therefore, *thermal deformations of the transmission case with coolant at 30°F below room temperature was within 100 μ-inches.*

IV. SUMMARY OF RESULTS

All the measured and calculated results are summarized in the table below:

Flatness Error Source	Major Source	Max. Error	Comment
Machine tool geometry	Spindle tilt	280 μin. ±70 μin.	indicator measure.
〃	〃	300 μin. ±50 μin.	plate cutting, stylus measure.
Forced deflections of the part	Axial cutting force	35 μin. ±15 μin.	static force-deflection test, proximity measure.
Thermal deformations of the part	Cutting heat	80μin.	dry cutting model, calculated
〃	〃	100 μin. ±25 μin.	dry cutting tests, thermocouple measurement
〃	Cold coolant	<100 μin.	cutting tests with coolant 30°F below room temperature, thermocouple measurement

p.s. The maximum step error of a transmission part milled in Ford's Livonia transmission plant is about 300 μ-inches (Figure 22).

From the results above, we found that ***the major error source contributing to the flatness problem is the spindle tilt of the machine tool.***

V. CONCLUSIONS AND RECOMMENDATIONS

1. The thermal and the force errors are of a different type than the spindle tilt errors. They are not only smaller in magnitude, but would not be expected to produce an error distribution with a step as shown in Figs. 9 or 22.

2. The error results reported here are for machining tests on a Fadal CNC 80 machining center at the U. M. However, by comparing Figs. 9 and 22 we might expect similar behavior on the machine at Ford's Livonia Transmission Plant. This should be investigated.

3. The measurement of spindle tilt using an indicator should be repeated in the transmission plant's machines so as to identify the existing spindle tilt of the machines used in production.

4. The magnitude of the spindle tilt required to produce an error of this magnitude is very small. The error is amplified due to the large diameter of the cutter (7.48"). It would be very expensive to acquire a more accurate machine tool. Reduction of the cutter diameter will reduce the production rate and , therefore is not recommended at this stage. Another approach is given below.

5. We recommend that a software compensation approach to be tried. The directions of tool motion programmed for the cutting contours could be changed to be parallel to the spindle

tilt direction on a particular machine so as to reduce the step error.

6. Coolant should be used at room temperature (or ideally 4°F below room temperature) so as to minimize the effect of thermal deformations. Coolant temperature control, although not required, might be desirable.

Appendix:

Specifications of the Transmission Case, the Finishing Cutter, and Cutting Conditions

AOD (or AODI) Transmission Case

	approximated dimension
length (inch)	15"
width (inch)	13"
height (inch)	3" ~ 6"
weight (lb)	33.5 lbs

Finishing Cutter

Diameter: 7.48" (190 mm)
No. of blades: 12

Cutting Conditions

feed (ipt)	.0034 (.086 mm/t)
cutting speed (sfm)	9791.5 (2984.5 m/min)
depth of cut (inch)	.02
spindle speed (rpm)	5000
feed (ipr)	.0409 (1.04 mm/rev)
feed rate (ipm)	204.7 (5200 mm/min)
feed stroke (inch)	40.79 (1036 mm)
machining time (sec)	12

References

[1] Boothroyd, G., Knight, W. A., 1989, "Fundamentals of Machining and Machine Tools", Marcel Dekker, Inc.

[2] Shaw, Milton C., 1984, "Metal Cutting Principles", Clarendon Press. Oxford. p251-p291.

[3] Kronenberg, M., 1966, "Machining Science & Application", Pergamon Press. p65-69, p147-156, p225-238.

[4] Fu, J. H., DeVor, R. E., Kapoor, S. G., Feb. 1984, "A Mechanistic Model for the Prediction of the Force System in Face Milling Operations", Journal of Engineering for Industry. Trans. ASME Vol.106, pp.81-88.

[5] Leist, T., Mar. 1990, "Test Program to Determine Cause of Flatness Problem in Valve Body Milling Operation", Defiance Proj. No. 1739.

[6] Chen, S. G., 1990 "Machining Error Diagnostics Using A Turning Process Simulator", Ph.D. Dissertation Proposal.

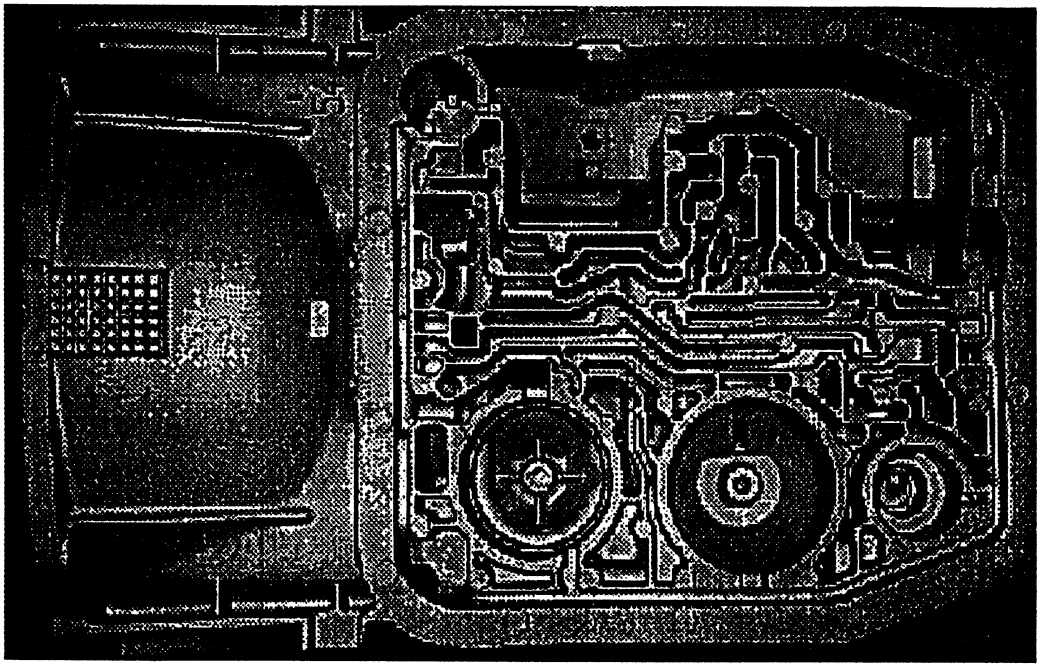

Figure 1: Top View of the AOD Transmission Case

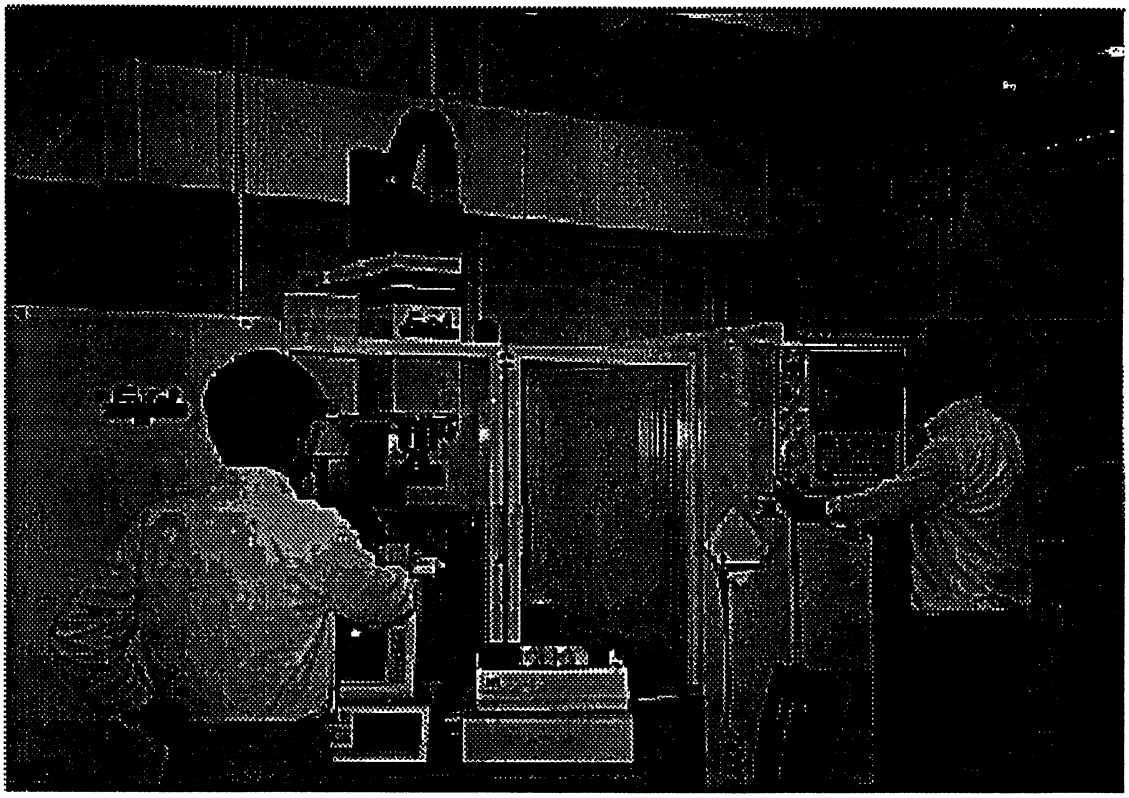

Figure 2: Machine Tool: Fadal CNC Milling Machine Center
(The University of Michigan, Ann Arbor, MI)

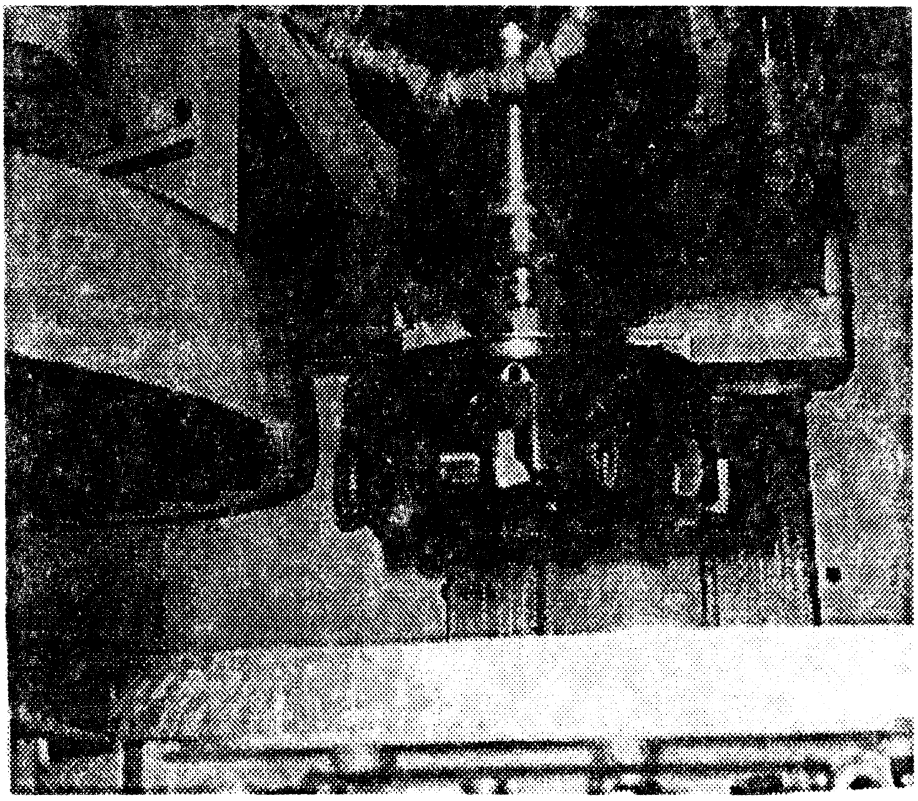

Cutter Diameter: 7.48" (190 mm)

Number of Blades: 12

Figure 3: Finishing Cutter

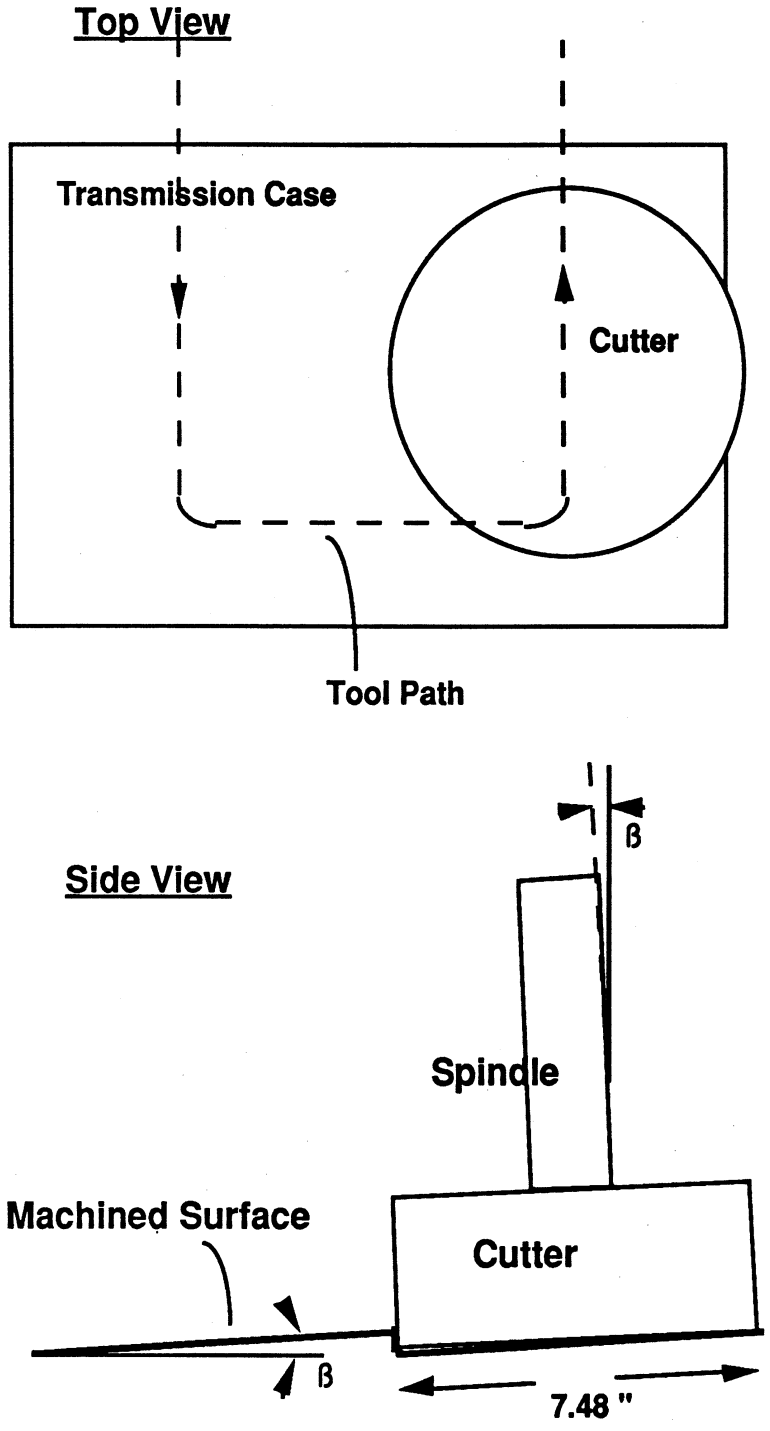

Figure 4: The Effect of Spindle Tilt on The Machining Flatness: The Spindle Tilt Will Cause a Step on the Machined Surface.

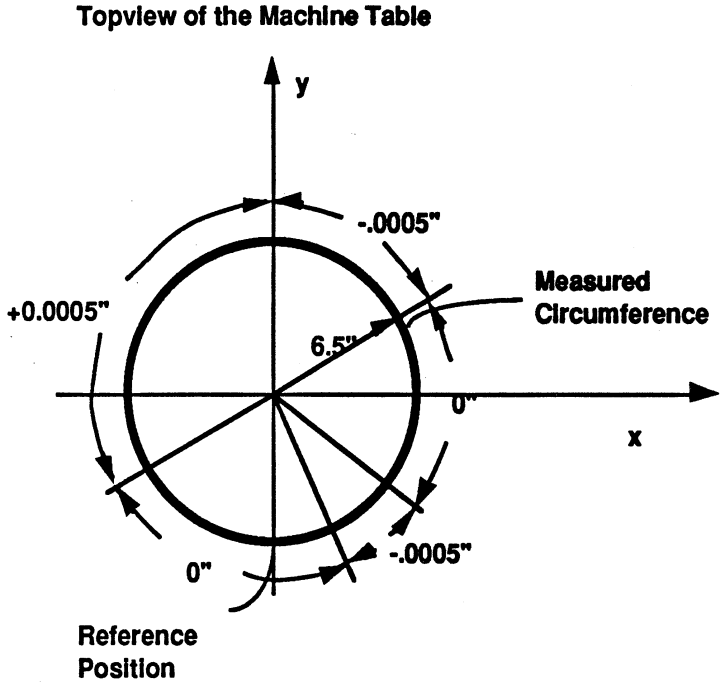

Figure 5: Analysis of Spindle Tilt Using a Dial-Gage Indicator with a measurement radius of 6.5 inches - The Measured results on Fadal CNC 80 Milling Machine Center

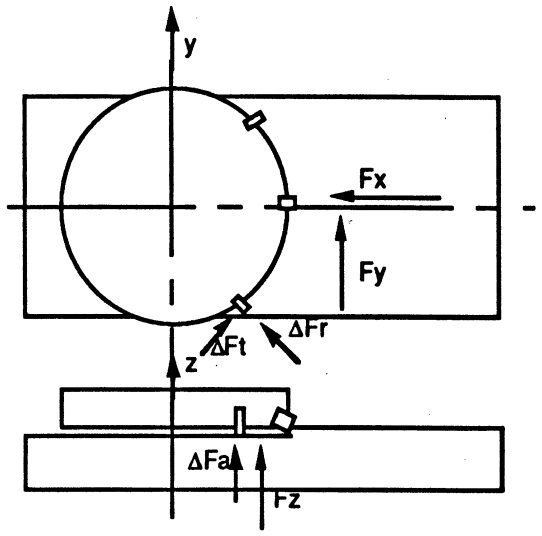

Figure 6: Milling Forces on a Flat Plate

Nomenclature

Fx: x-direction force component acting on the cutter

Fy: y-direction force component acting on the cutter

Fz: z-direction force component acting on the cutter

(total cutting force =square root of $(Fx^2+Fy^2+Fz^2)$

ΔFr: radial force component of one insert

ΔFt: tangential force component of one insert

ΔFa: axial force component of one insert

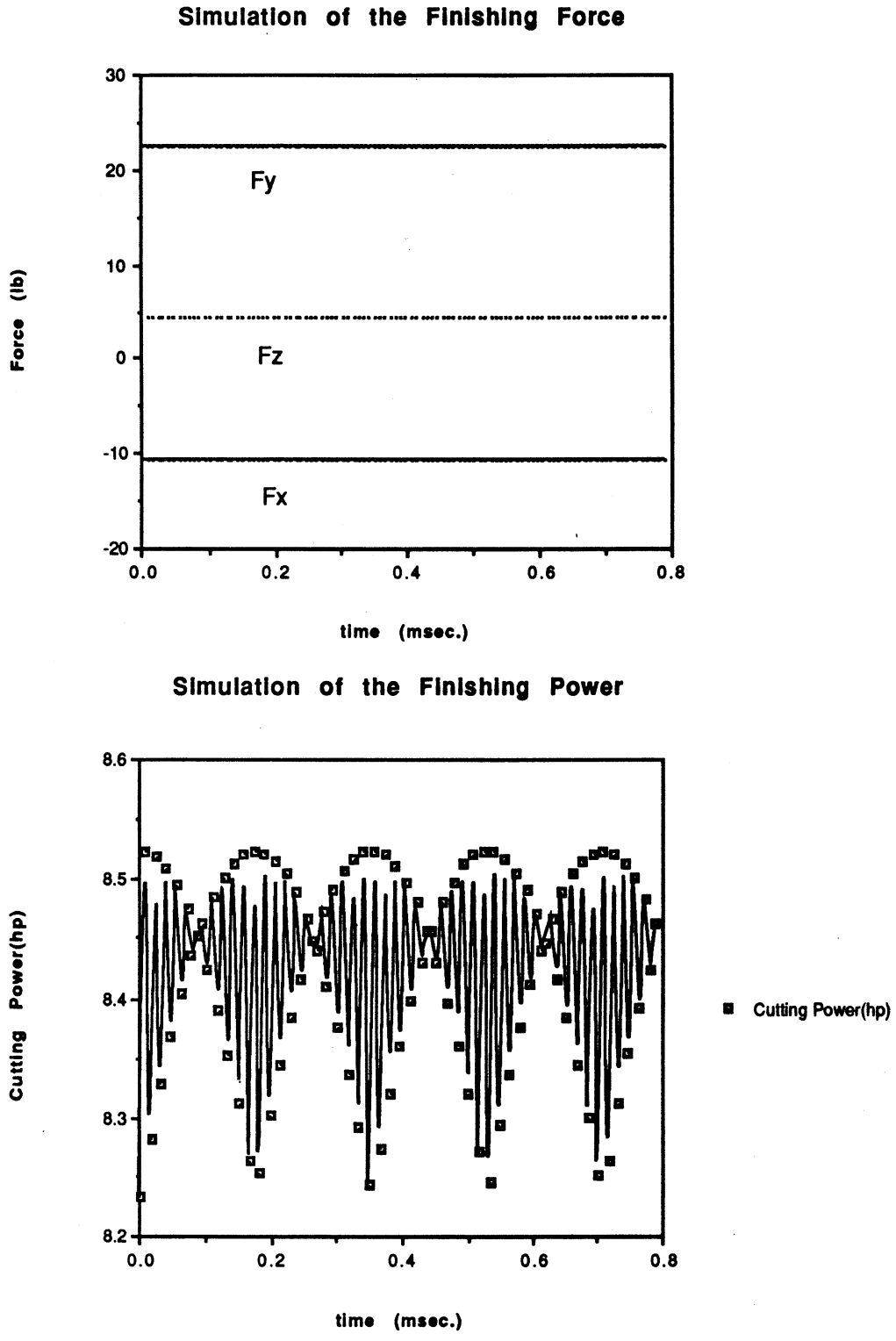

Figure 7: Simulation of the Finishing Force and Power

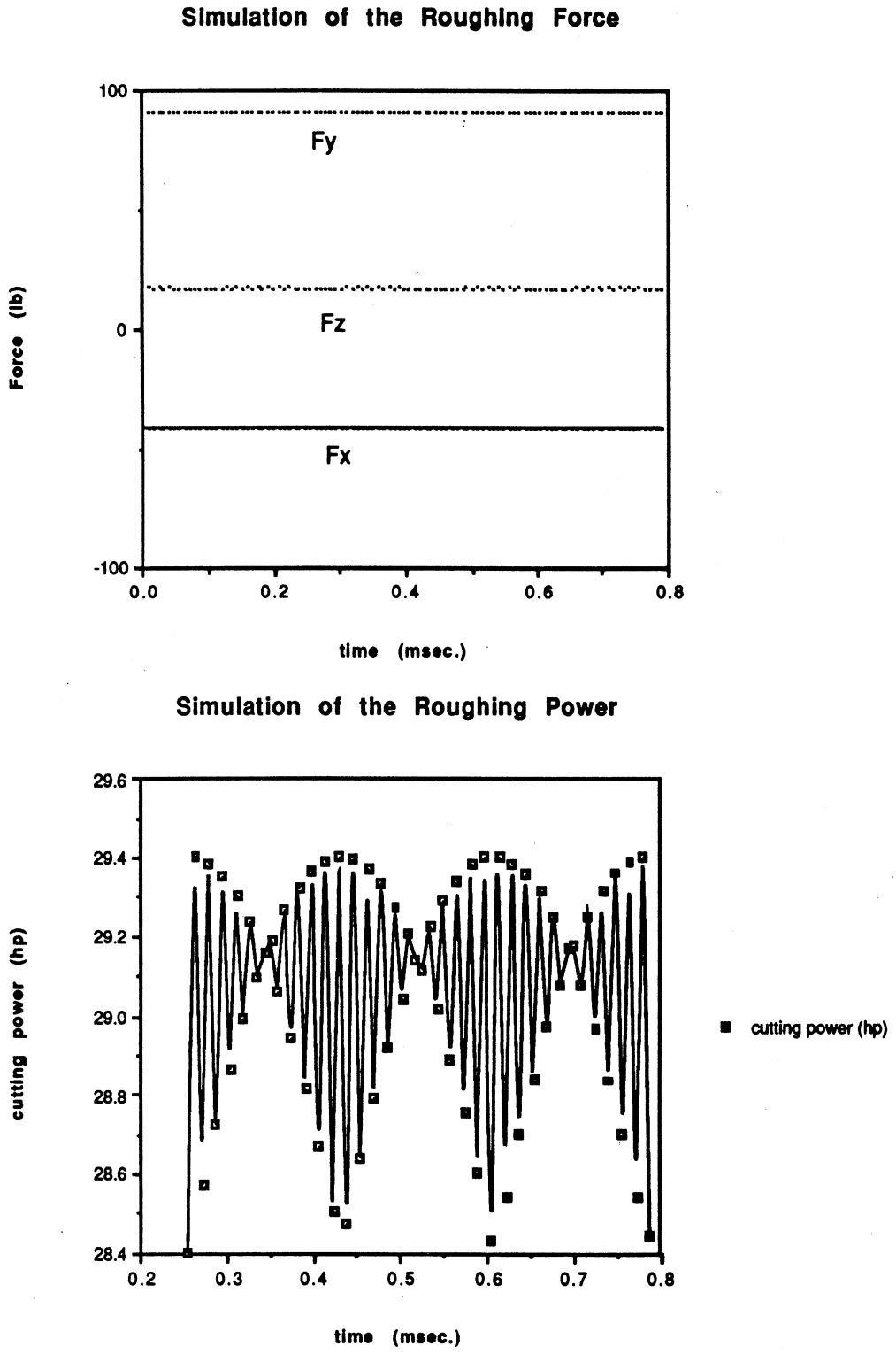

Figure 8: Simulation of the Roughing Force and Power

Top View

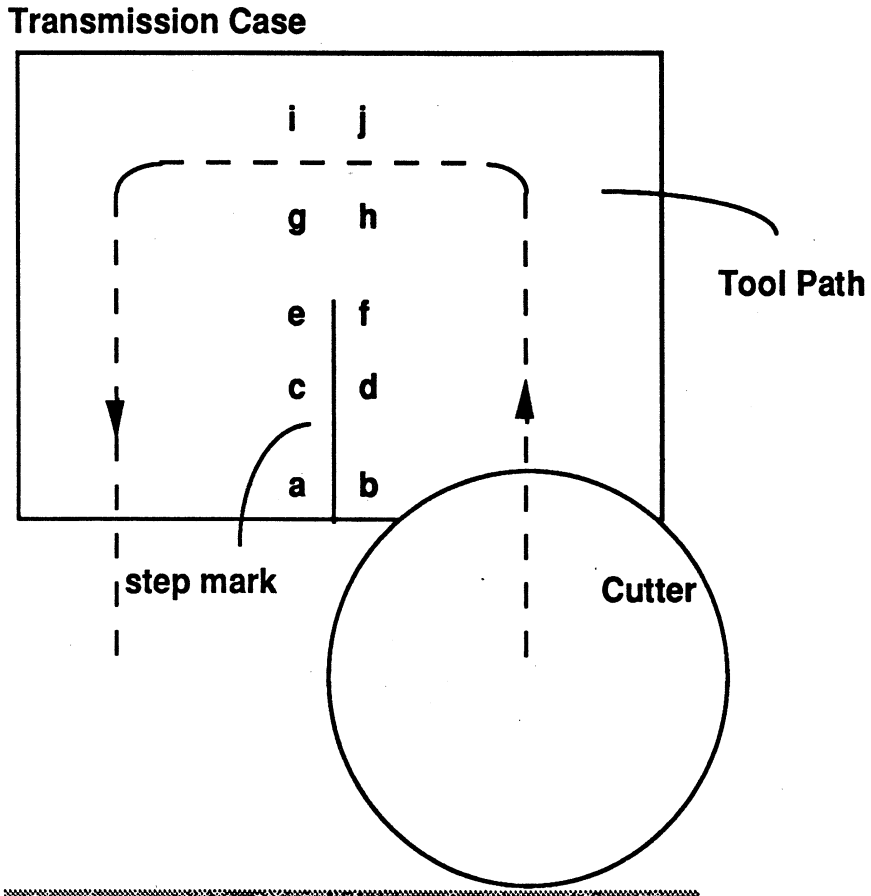

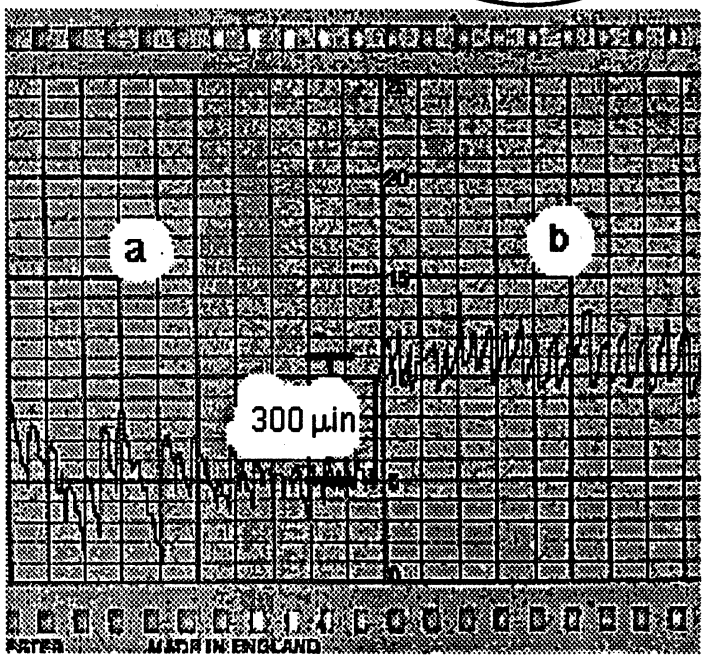

Figure 9: Plate Flatness Measurement.
(Maximum step error was at a-b line: 300 ±50 µinches.)

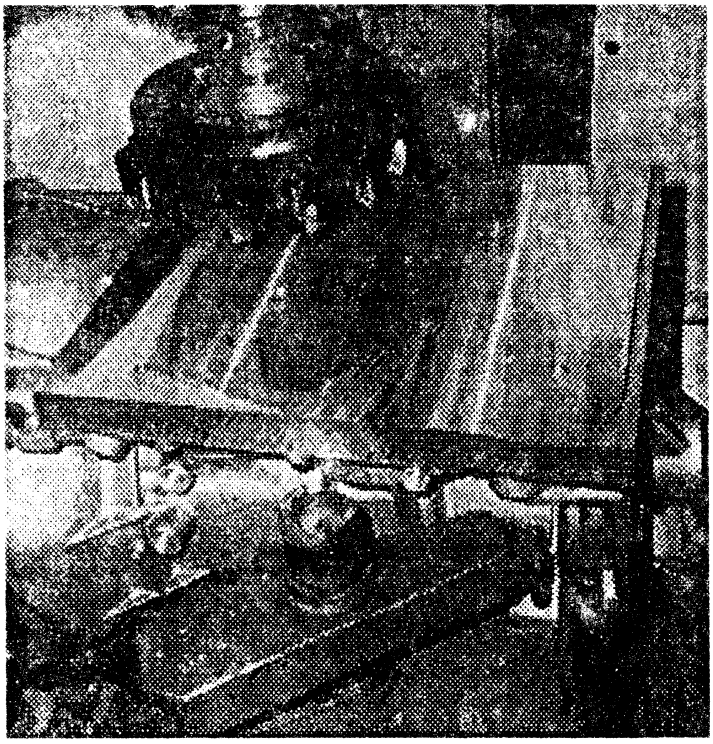

Figure 10. Mill a Flat Plate Mounted on Top of the Transmission Case

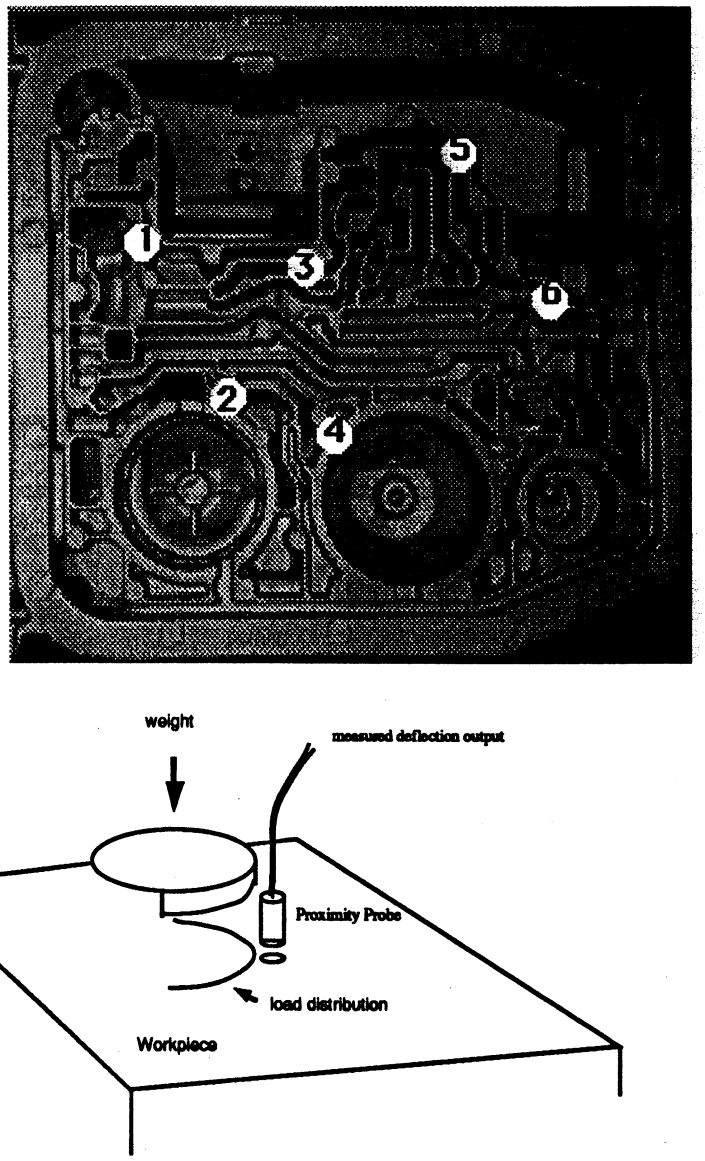

Figure 11: Schematic of the Static Force-Deflection Experiment

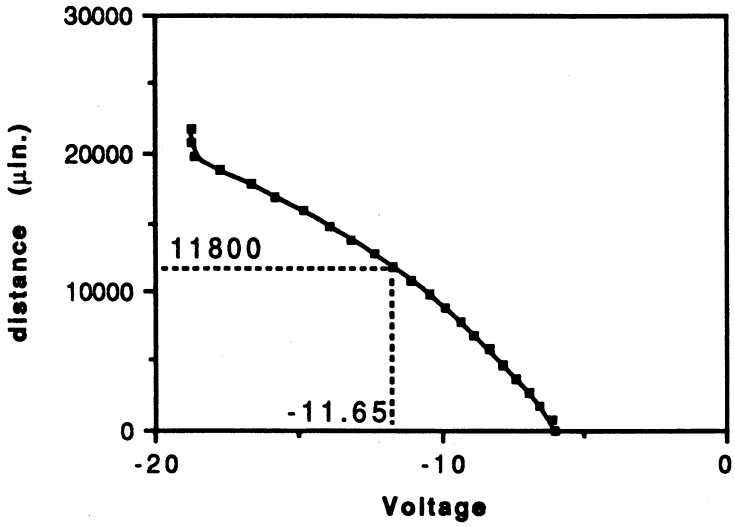

Sensitivity: 6.75* 10-4 $\frac{\text{Volts}}{\mu\text{-inches}}$

Figure 12: Calibration of the Proximity Sensor

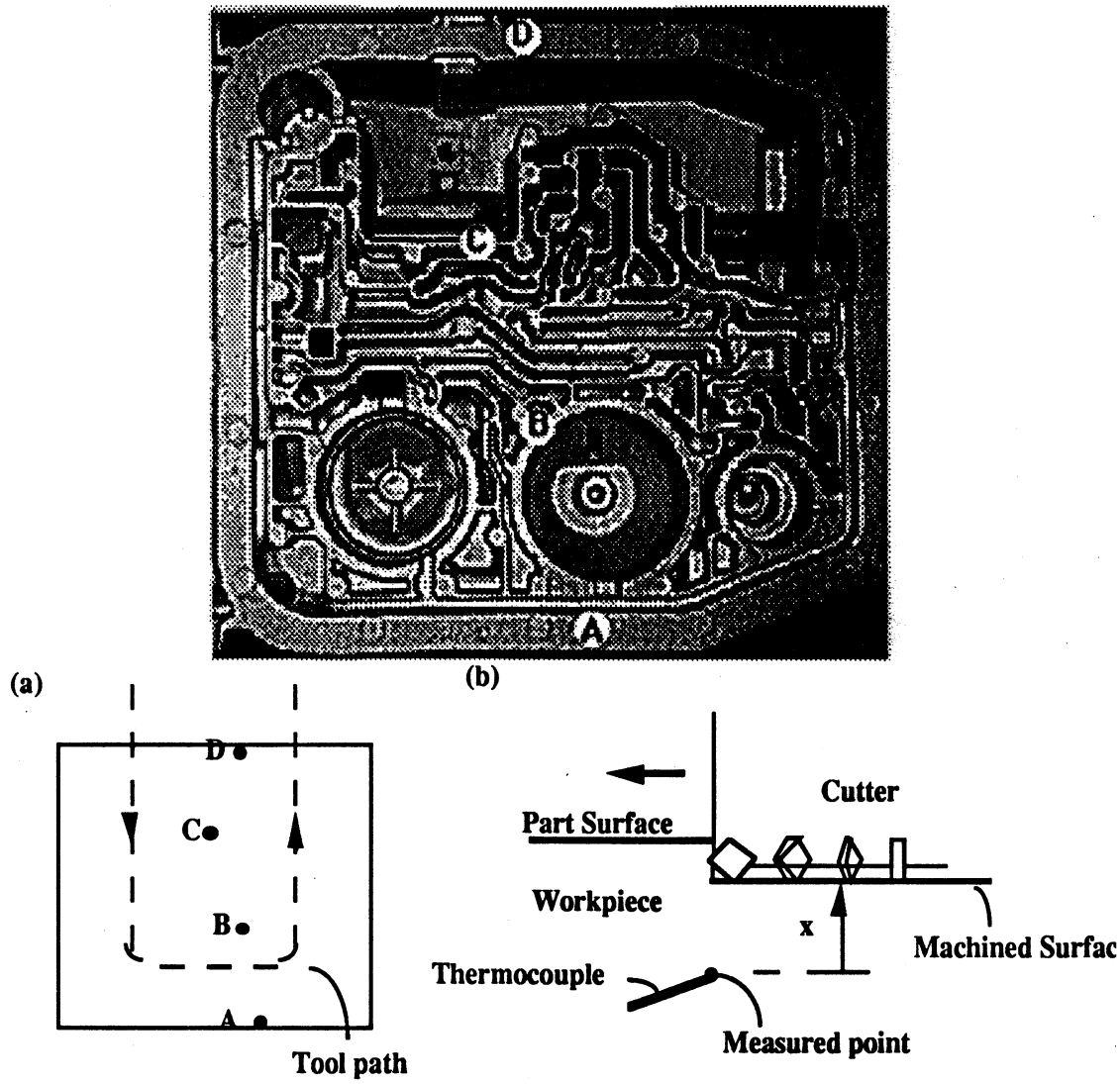

Figure 13: Experimental Design of the Cutting Temperature Measurement. (a) Top view of the machined surface. (b) The distance x between the measured point and the machined surface

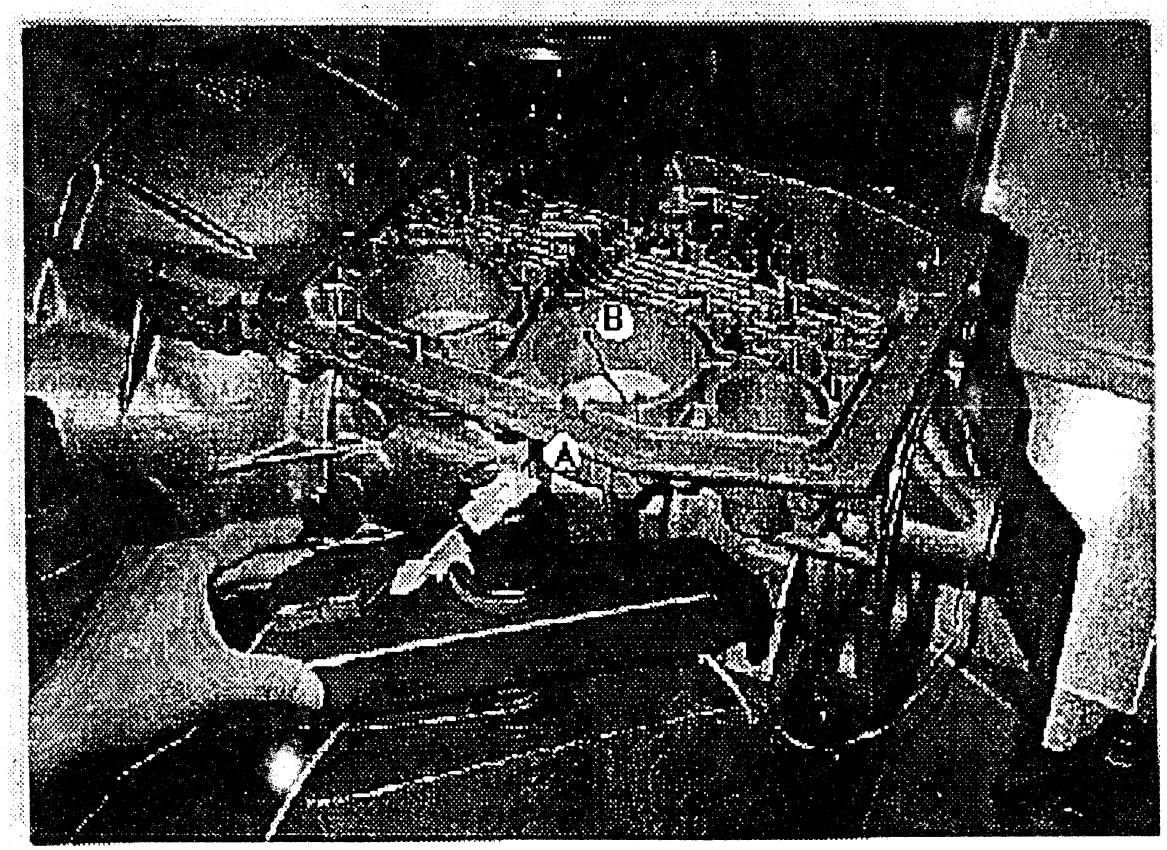

Figure 14: Setup of Thermocouples on the Transmission Case

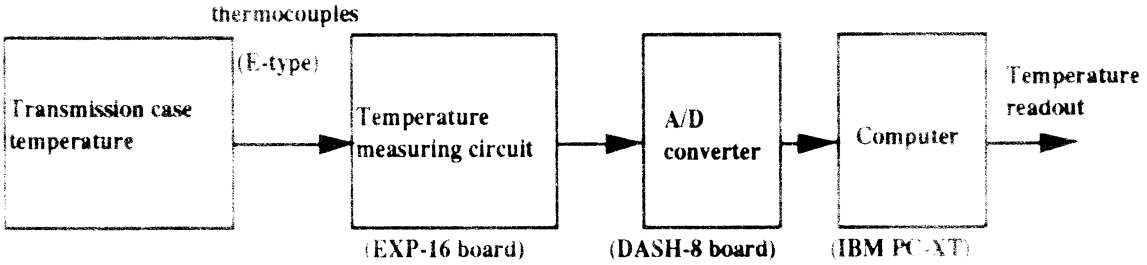

Figure 15. Setup of the Data Acquisition System for the Temperature Measurement

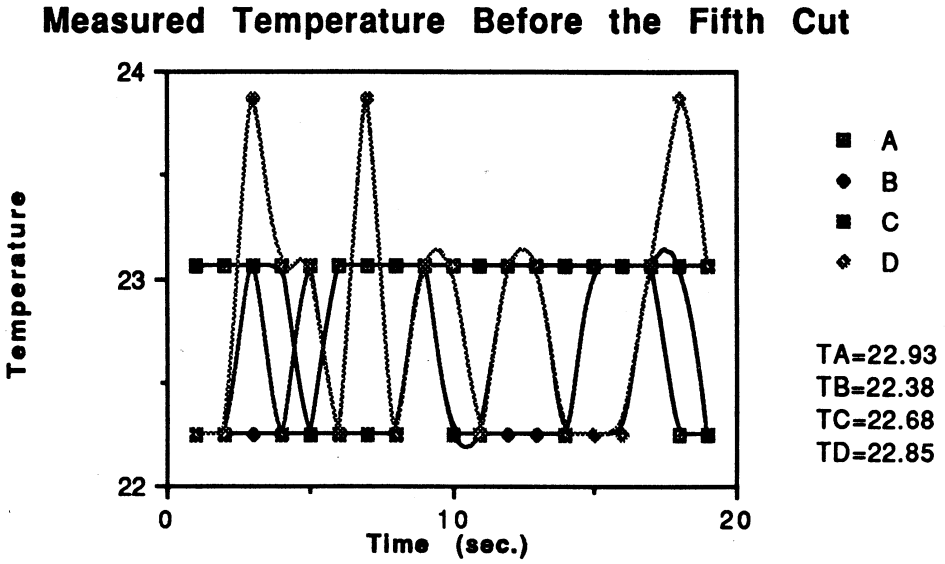

Resolution: about 1°C

Figure 16: Resolution of the Data Acquisition System: Typical Measured Transmission Case Temperatures Before Cutting.

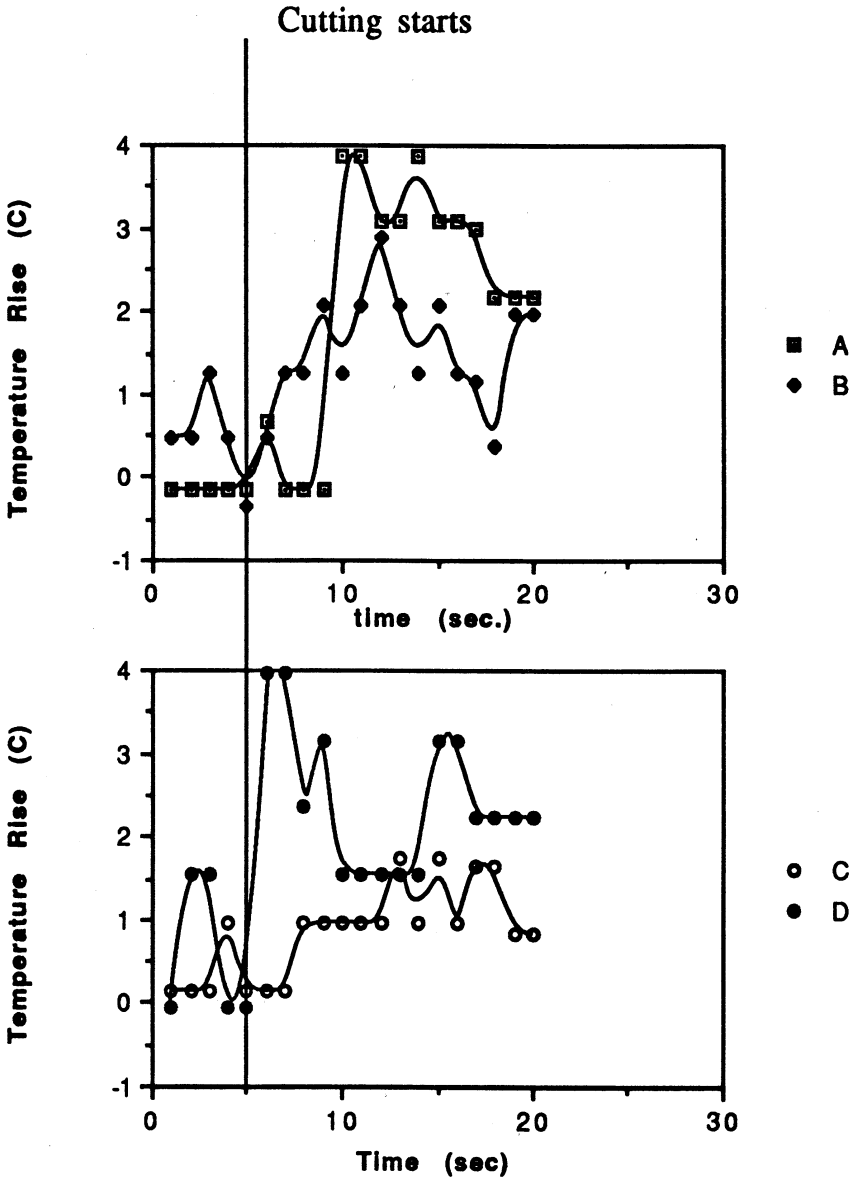

Figure 17: Typical Measured Temperatures for Dry Cutting

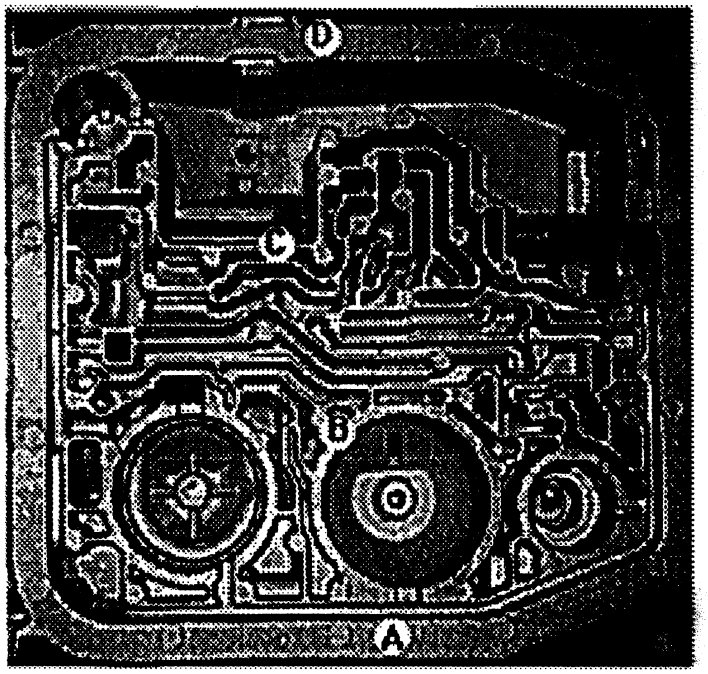

(a)

(b)

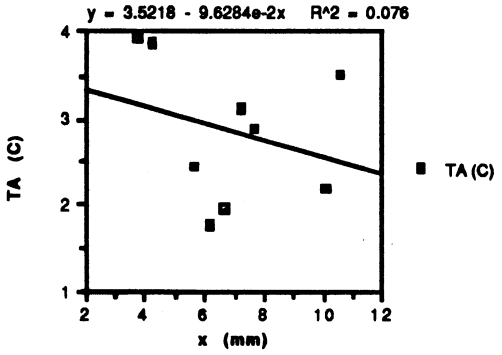

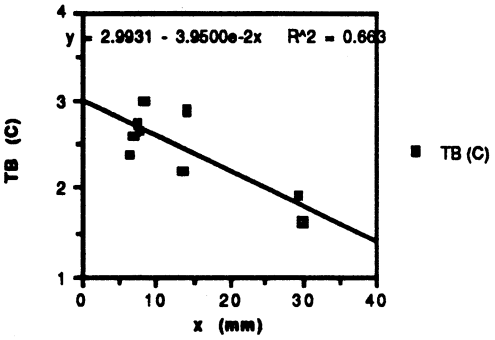

(c)

(d)

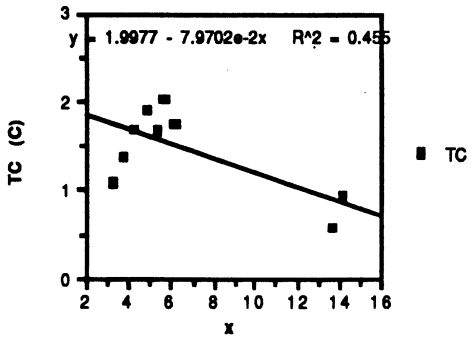

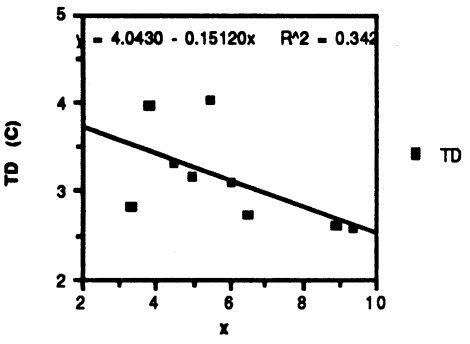

Figure 18: Temperature Distribution for Dry Cutting

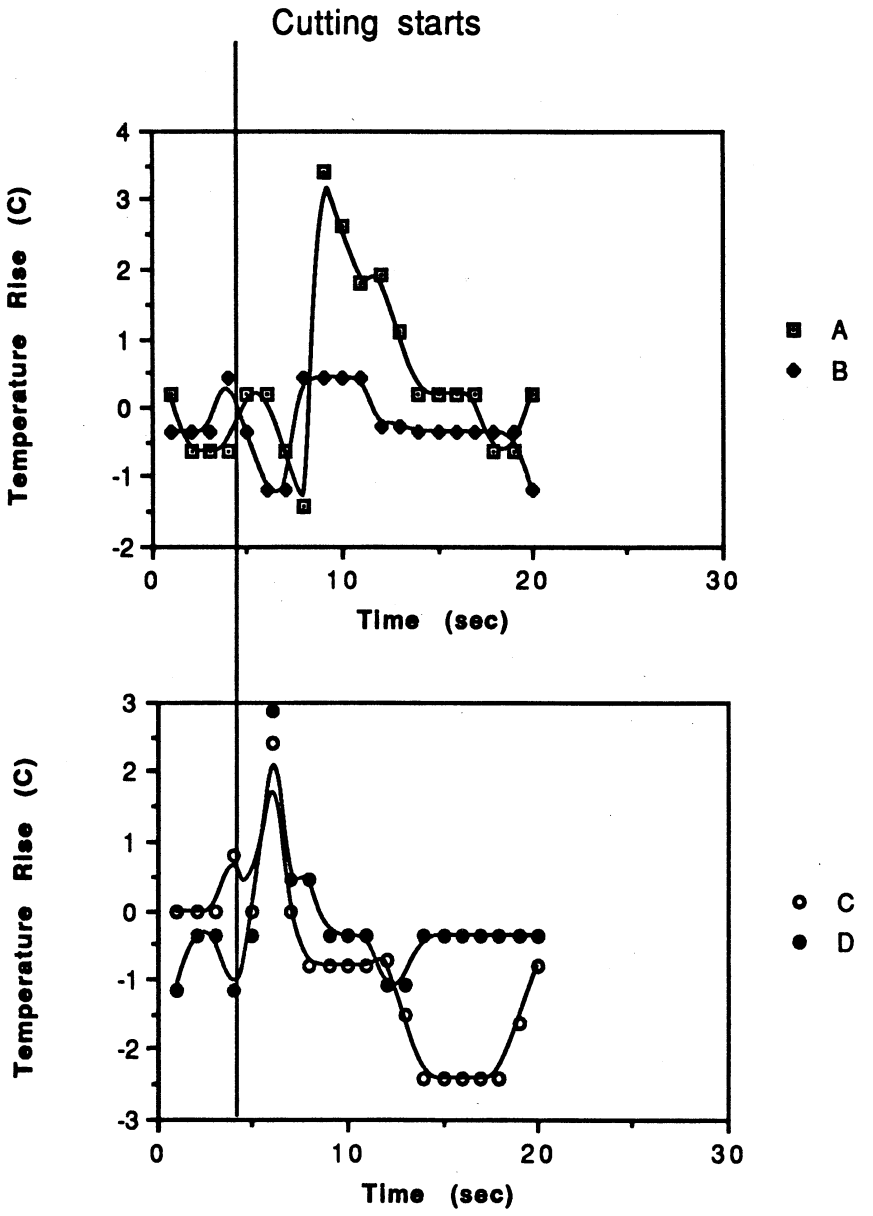

Figure 19: Typical Measured Temperatures for Cutting with Coolant at Room Temperature

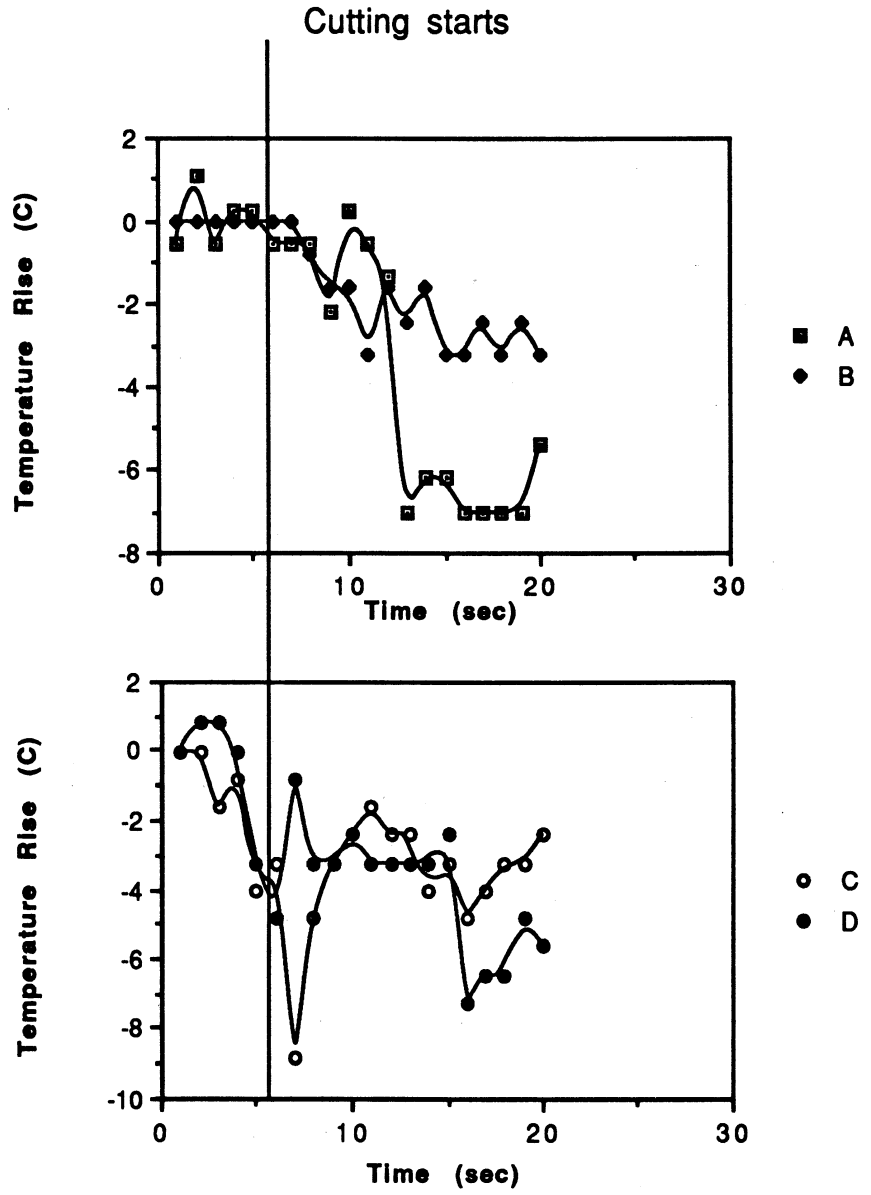

Figure 20: Typical Measured Temperatures for Cutting with Coolant 30°F below Room Temperature

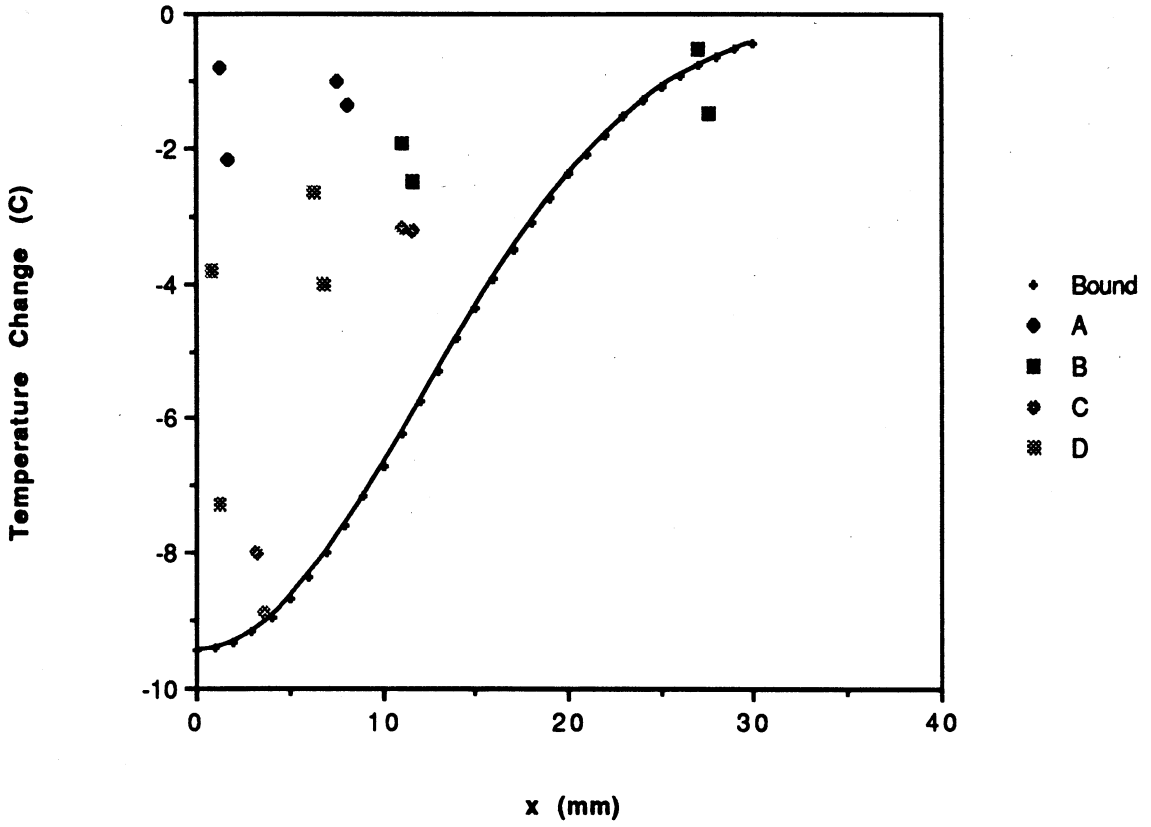

Figure 21: Temperature Distribution for Cutting with Coolant 30°F below Room Temperature

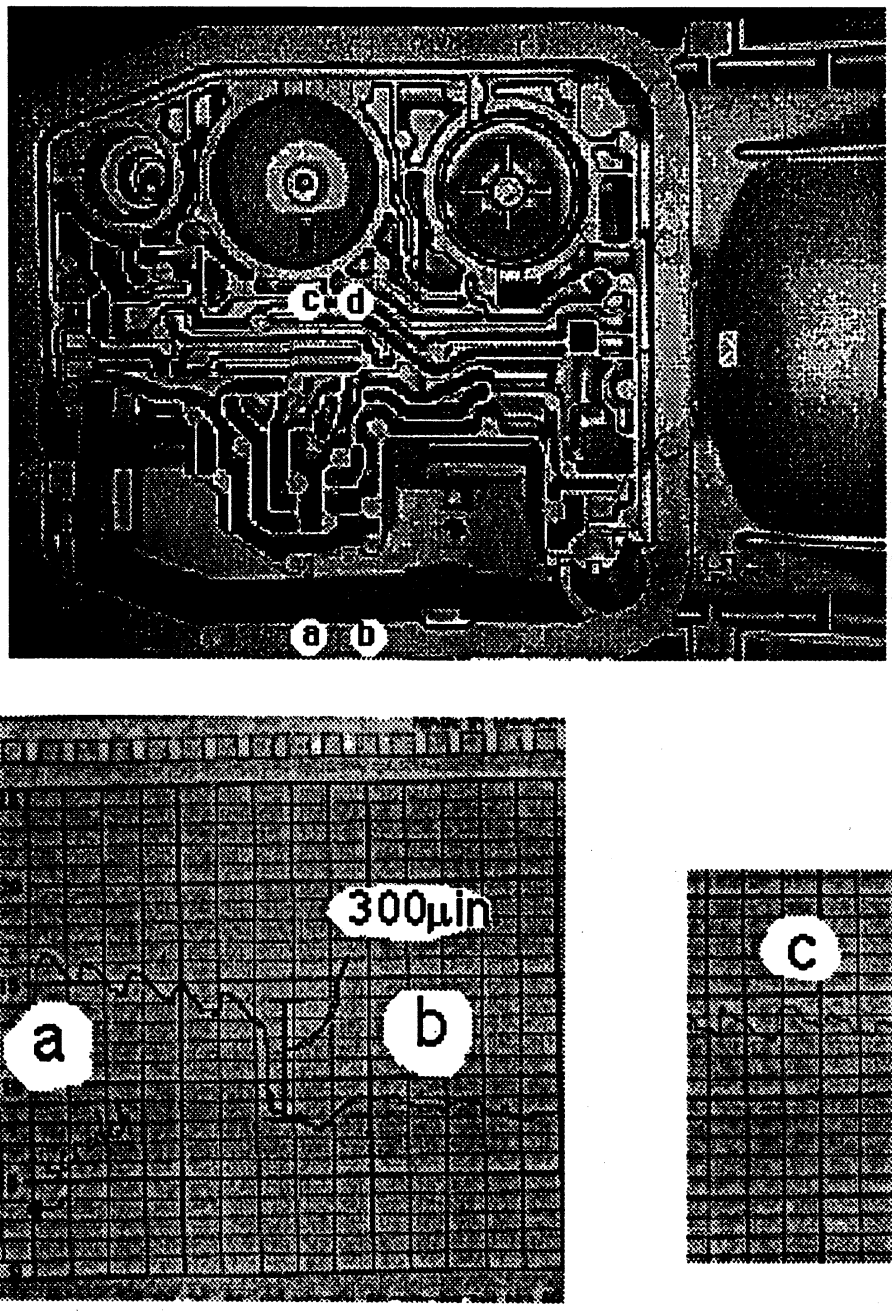

Figure 22: Profile of the Face-Milled Surface of the Transmission Case at Ford Transmission Plant in Livonia, Michigan